Performance and mechanism of the separation of C8 α-olefin from F-T synthesis products using novel Ag-DES

Hu Li[1] | Zisheng Zhang[1,3] | Guanlun Sun[1] | Suli Liu[2] | Liangcheng An[2] | Xingang Li[1] | Hong Li[1] | Xin Gao[1,*]

[1]School of Chemical Engineering and Technology, National Engineering Research Center of Distillation Technology, Collaborative Innovation Center of Chemical Science and Engineering (Tianjin), Tianjin University, Tianjin 300072, China

[2]Ningxia Coal Industry Group Co. Ltd., CHN ENERGY, Yinchuan 750011, PR China

[3]Department of Chemical and Biological Engineering, University of Ottawa, Ottawa K1N 6N5, Canada

Corresponding author

Xin Gao, School of Chemical Engineering and Technology, National Engineering Research Center of Distillation Technology, Collaborative Innovation Center of Chemical Science and Engineering (Tianjin), Tianjin University, Tianjin 300072, China.

Email: gaoxin@tju.edu.cn

Funding information

National Key R&D Program of China, Grant/Award Numbers: 2018YFB0604900; Key Research and Development program of Ningxia, Grant/Award Numbers: 2018BDE02057

Abstract: As an attractive alternative technology for the separation of long chain olefin and paraffin, a novel silver-based deep eutectic solvent (Ag-DES) was prepared and utilized for 1-octene/n-octane separation. Comprehensive reactive extraction separation experiments were performed to highlight the Ag-DES concentration and operating temperature discriminations using compounds with different ratio of 1-octene/n-octane. The novel Ag-DES showed optimal separation performance regarding 1-octene/n-octane and possessed the highest levels separation selectivity in the range 3.75-16.74 with excellent circulation stability in our best knowledge. Furthermore, FT-Raman measurements and quantum chemistry calculation were conducted to elucidate the interaction mechanism of Ag-DES in the separation of 1-octene and n-octane, which revealed that both chemical complexation and strong physical attraction existed in the complex of Ag-DES with 1-octene rather than n-octane. This study lends important insight for the development of Ag-DES reactive extraction separation process for the energy-efficient long chain α-olefin purification from F-T synthesis products.

KEYWORDS

silver-based deep eutectic solvent, reactive extraction, separation, 1-octene, α-olefin

1 | INTRODUCTION

Long chain α-olefins have extremely high added-value, which are widely used as co-monomers for polymers such as polyethylene, the synthesis of halogenated hydrocarbons, and oligomerization to lubricating oils, etc.[1] At present, the production of long chain α-olefins

in industry is mainly obtained from ethylene oligomerization and separation from Fischer-Tropsch stream.[2,3] Although the former process is simple, the heavy byproducts are serious and cost much more money.[4] The liquid products of Fischer-Tropsch synthesis are valuable raw materials for the separation of long chain α-olefins because of the relatively higher content of α-olefins with carbon number of 6–25,[5] whereas they are used as low-value fuels at present. The α-olefins separated from Fischer-Tropsch synthesis products are a commercially valuable class of chemical compounds. However, the separation process is currently one of the most energy-intensive and costly processes in the petrochemical industry, because of the structural similarity and lower relative volatility between olefins and paraffins with the same carbon number.

A series of researches were focused on the purification of α-olefins from olefin/paraffin mixtures including with 1-octene/n-octane. Distillation method is an energy- and capital-intensive scheme required a plurality of columns, a large number distillation trays and higher reflux ratio.[6] Physical and chemical adsorption were rarely employed to separate liquid α-olefins with the difficulty in determination of adsorption capacity.[1,7] Facilitated transport membrane containing transition metal has been widely studied and applied in the separation of olefin/paraffin recent years, especially silver ion and cuprous ion.[8,9] The chemical complexation between the transition metal cations and the double bond of olefin can effectively achieve the selective separation of α-olefins.[10] Liu et al.[11] and Rychlewska et al.[12] obtained extremely high permeability and separation selectivity in the separation of 1-hexene/n-hexane and 1-octene/n-octane mixtures due to the dissolution and diffusion differences on the facilitated transport membrane. However, it is limited to large-scale application because

of low transported capacity and high cost.[13] Considering the above processes with various problems, it is of great necessity to develop an alternative technology with a good selectivity for α-olefins, eco-efficiency, stable physicochemical properties, easy recovery and pollution-free. As a green designable solvent, deep eutectic solvents (DESs) and ionic liquids (ILs) have these characteristics.[14,15] Among them, transition metal-based deep eutectic solvent is a more promising reactive extractant for the separation of α-olefins with great application potential.

A deep eutectic solvent is a fluid mixture composed of two or more safe components through hydrogen bonds with lower melting point than any of their individual component.[16,17] Compared with the traditional solvent ILs, most of DESs exhibit a lot of remarkable advantages such as desirable biodegradability, environmental friendliness, ease of preparation for large-scale applications and show great interests in many fields.[16,18] DESs have been widely used in the extraction separations,[18] natural products extraction,[19] gasouse mixture separations,[20,21] catalysis,[22,23] dissolution and modification processes,[24] electrochemistry[25] and material chemistry.[26] Jiang et al.[27,28] have achieved a good separation selectivity in the separation of ethylene/ethane with DESs as supported liquid membranes. However, there are almost no researches to report the application of DESs in the separation of liquid α-olefins, such as 1-hexene/n-hexane and 1-octene/n-octane. Nevertheless, the olefin-to-paraffin selectivity in pure ILs and DESs without transition metal is very low.[13,14] Considering the chemical complexation between the transition metal cations and double bond of olefin, the addition of silver-based cation can greatly improve the olefin selectivity and separation efficiency. Therefore, to design and prepare silver-based DESs to enhance olefin-to-paraffin

selectivity is of great necessity. The study of interaction mechanism is favorable to optimizing the extractant structure and further improving the separation performance.

Based on these reasons, we designed and prepared a novel sustainable silver-based deep eutectic solvent (Ag-DES) consisted of N,N-dimethylbenzamide (DMBA) and silver trifluoromethanesulfonate ($AgCF_3SO_3$). The structure of Ag-DES was characterized by FT-IR, FT-Raman, ^1H NMR, and ESI-MS. The effect of olefin concentration, molar ratio of Ag-DES to 1-octene, operating temperature on the distribution coefficient and the selectivity of olefin to paraffin were investigated in the binary 1-octene/n-octane mixture. The long-term stability of the Ag-DES was evaluated by repeated circulation stability experiments. In addition, quantum chemistry calculation was carried out by using Gaussian 09 software package based on density functional theory (DFT) to calculate the optimized geometries, interaction energies, combined the measurements results from FT-Raman to analyze the intermolecular covalent and non-covalent interactions and reveal the interaction mechanism of Ag-DES with 1-octene and n-octane. In particular, this study will provide a novel insight for the role of Ag-DES for separation of the long chain olefins/paraffin, which is of great help for us to screen new Ag-DES for separation of α-olefins from F-T synthesis products.

2 | EXPERIMENTAL SECTION

2.1 | Materials and reagents

1-octene (> 98 wt.%) was purchased from Shanghai Maclean Biochemical Technology Co., Ltd. (Shanghai, China). n-octane (> 99 wt.%) was purchased from Tianjin Jiangtian Chemical Technology Co., Ltd. (Tianjin, China). N,N-dimethylbenzamide (DMBA, > 99.9 wt.%) was provided by Shanghai Aladdin Biochemical Technology Co., Ltd. (Shanghai,

China). Silver trifluoromethanesulfonate ($AgCF_3SO_3$, ≥ 99.8 wt.%) was supplied by Shanghai Haohong Biomedical Technology Co., Ltd. (Shanghai, China). All chemicals were used as received without further purification.

2.2 | Preparation of Ag-DES

A certain amount of $AgCF_3SO_3$ was dried under the light-protected vacuum conditions at 65°C for 24 h, and then taken out and placed in a vacuum desiccator in a dark place. The Ag-DES was prepared by mixing DMBA and $AgCF_3SO_3$ with a certain molar ratio of 2:1 and then placed in a dark environment with a 60°C constant temperature oil bath for heating and stirred with an electronic digital display stirrer at 200 rpm for 1 h to form a homogeneous light yellow liquid. The synthetic route is shown in Scheme S1.

2.3 | Characterizations of Ag-DES

Physical property measurements mainly contain viscosity, density and thermal stability. The kinetic viscosity of the Ag-DES was tested at atmospheric pressure with the DV-III+ digital viscometer. The density of the Ag-DES was measured with the measuring cylinder and the electronic balance. Each sample was examined three times to obtain an average value under the same conditions. DTG-60AH was used for thermogravimetric analysis as a detector to place the sample on an aluminum pan under a nitrogen atmosphere. The temperature started from room temperature to a final temperature of 600°C with an increasing rate of 10°C/min. The chemical structure of Ag-DES was investigated by using FT-IR, FT-Raman, ^1H NMR and EIS-MS. The interaction mechanism of Ag-DES with 1-octene and n-octane was recorded by using FT-Raman spectroscopy with a 785 nm laser.

2.4 | Reactive extraction experiments

According to the certain concentration gradient, a series of mixtures of 1-octene and n-octane were sequentially prepared with the same weight, which were introduced into multiple 100mL crystallizers. The experimental apparatus is as shown in Figure 1. Ag-DES was added into these crystallizers with the same volume and composition in a dark environment. The vessel was properly wrapped for the light-protection of Ag-DES to avoid quality deterioration and fixed in a thermostatic bath to maintain a constant temperature of $T = 298.15 \pm 0.5$K. The ternary mixtures were stirred for 1 h under the speed of 200 rpm to reach the thermodynamic equilibrium and then settled at the same temperature for 1h to get the phase separation. The samples in organic phase were taken out by buret without disturbing the phase boundary and weighed. The reactive extraction experiments for investigating the effect of olefin concentration, molar ratio of Ag-DES to 1-octene and temperature for the ternary biphasic system were performed with the conditions shown in Table 1. Five times of circulation experiments were carried out under the same conditions, which were determined according to the TGA results for the complex of Ag-DES with 1-octene as shown in Figure S1. The complex was rotated evaporation for 12 h at a constant temperature of 65°C and depressurized at a low pressure about 10 kPa.[29] The procedure was consistent with the previous description of extraction equilibrium experiments.

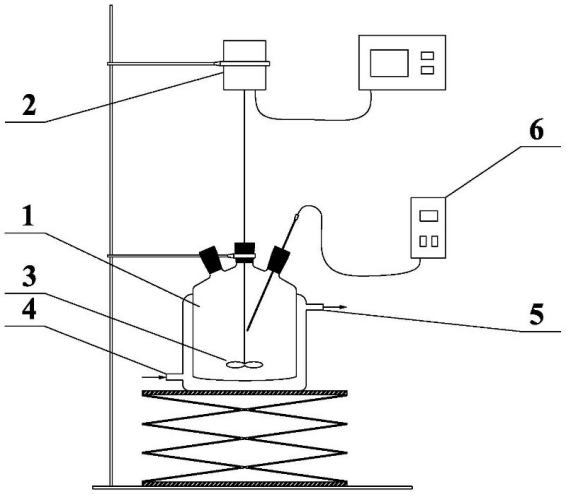

FIGURE 1 Experimental apparatus for reactive extraction. 1- crystallizer, 2- digital display electric stirrer, 3- propeller, 4- heat-transfer medium inlet, 5- heat-transfer medium outlet, 6- digital thermometer

TABLE 1 The operating conditions for reactive extraction experiments on the effect of olefin concentration (c_1), molar ratio of Ag-DES to 1-octene (n_{Ag}/n_1), temperature (T) and circulation stability for the ternary biphasic system

Effects	**Mass of Ag-DES/g**	**Mass of C8/g**	c_1**/wt.%**	n_{Ag}/n_1	T**/°C**
Olefin concentration	11.106	4.48	10/30/50/70/90	——	25
Molar ratio of Ag-DES to 1-octene	11.106	6.72	50	1:1/1:1.5/1:2/1:2.5/1:3	25
Temperature	11.106	6.72	50	1:1.5	0/10/20/25/30/40
Circulation stability	11.106	6.72	50	1:1.5	25

2.5 | GC analysis

The content of each component in the organic phase was analyzed by the PE Auto System XL Gas Chromatograph with a HP-5 non-polar chromatography column (0.32 mm × 30 m × 0.25 μm, Agilent). The content of each component in the two phases was calculated by conservation of mass as the following equations. The mass of raw material (M) was calculated using Equation (1). Subscripts 1, 2 and 3 represent 1-octene, n-octane and Ag-DES, and superscripts org and sol represent organic phase and Ag-DES solvent phase, respectively.

$$M = m_1 + m_2 + m_3 = M^{org} + M^{sol} \quad (1)$$

where m_1, m_2 and m_3 are the mass of 1-octene, n-octane and Ag-DES, M^{org} and M^{sol} stand for the total mass of organic phase and solvent phase, respectively. After the extraction equilibrium experiment, the total mass of the organic phase M^{org} and solvent phase M^{sol} can be expressed by Equations (2) and (3), respectively.

$$M^{org} = m_1^{org} + m_2^{org} + m_3^{org} \quad (2)$$

$$M^{sol} = m_1^{sol} + m_2^{sol} + m_3^{sol} = M - M^{org} \quad (3)$$

M^{org} can be separated and weighed. The mass fractions of solute in the organic phase (x_1^{org} , x_2^{org}, $x_3^{org} = 1 - x_1^{org} - x_2^{org}$) can be obtained by GC analysis and then the mass of each component in both the two phases can be calculated by Equations (4) and (5). The content of each component in solvent phase can be donated by Equation (6).

$$m_i^{org} = M^{org} x_i^{org} \ , \ (i=1,2,3) \quad (4)$$

$$m_i^{sol} = m_i - m_i^{org} \ , \ (i=1,2,3) \quad (5)$$

$$x_i^{sol} = m_i^{sol} / M^{sol} \ , \ (i=1,2,3) \quad (6)$$

2.6 | Simulation details

The density functional theory (DFT) quantum chemistry calculation method was employed for the analysis of Ag-DES, hydrocarbons and their complexes. All the geometric configurations were optimized by using Gaussian 09 software.[30] An ab initio calculation was performed with the M062X[31] method and def2tzvp basis set[32] by full optimization of energies and calculation of vibrational frequencies without any geometrical constraints. The solvent effect was considered because of its electrostatic impact on the geometries of cations and anions. There was no imaginary frequency in all of geometries and the zero-point vibrational energies (ZPEs) were also obtained for the calculation of the interaction energies between the Ag-DES and olefin/paraffin. Electron density and structural characteristics in terms of atomic components were quantitatively analyzed by multiwfn.[33] A series of weak interactions of intermolecular were qualitatively depicted by the isosurfaces of reduced density gradient function (RDG).[34] Furthermore, the covalent and strong non-covalent interactions between intermolecular were recorded and distinguished by the topological parameters at bonding critical points (BCPs) of Atoms in Molecules (AIM).[35] Furthermore, Aspen Plus 8.4 was employed to analyze the energy consumption on the separation of 1-octene and n-octane.

3 | Ag-DES CHARACTERIZATIONS

3.1 | Thermal stability

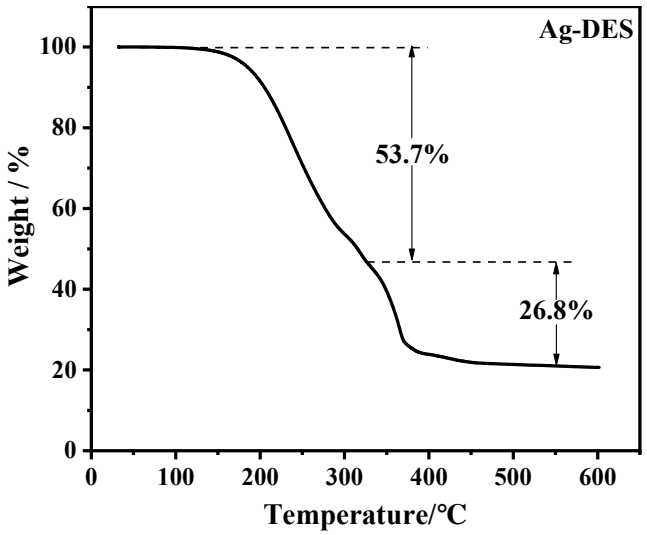

FIGURE 2 Scanning thermal gravimetric analysis (TGA) for Ag-DES with a 10°C /min heating rate under the nitrogen atmosphere

TGA was conducted to examine the thermal stability of the Ag-DES. As shown in Figure 2, Ag-DES remained stable at a relatively low temperature and began to decompose until the temperature reached 160°C. An overall mass loss about 54% started at 160°C and finished at about 330°C, which can be ascribed to the removal of DMBA. The second mass loss from 330°C to about 550°C is attributed to the decomposition process of silver trifluoromethanesulfonate. Finally, a residual mass fraction of about 20% is the involatile silver in the Ag-DES. In addition, a cooling process for stirless Ag-DES from 25°C to -20°C in 40 minutes was carried out to test its tolerance under low temperature. The fluidity gradually declined with the decreasing of temperature until loss of mobility at less than -5°C. There was a tendency to convert the solid when the temperature was further reduced after -20°C. Therefore, it can be concluded that it has a better thermal stability and a wide liquid

range from -5°C to 160°C. The viscosity and density of the Ag-DES are 170.25 cP and 1.395 g/mL at room temperature, respectively.

3.2 | Chemical characterizations

The chemical structure of Ag-DES were recorded by using FT-IR, FT-Raman, 1H NMR and EIS-MS, which were mainly concentrated on the chemical complexation between silver ion and the carbon-oxygen double bond of DMBA as shown in Figure S2 and the destruction and reconstruction of hydrogen bonds in the synthesis of Ag-DES as shown in Figure S3. Both of them illustrate the successful preparation of Ag-DES.

4 | α-OLEFIN SEPARATION PERFORMANCE

In this study, Ag-DES was utilized as reactive extractant for the separation of α-olefins in the 1-octene/n-octane mixture. The separation performance was evaluated by the distribution coefficient of solute *i* (D_i) and the selectivity of solute *i* to solute *j* ($S_{i,j}$), both of them were calculated by using Equations (7) and (8)[13]:

$$D_i = \frac{x_i^{sol}}{x_i^{org}}, (i = 1,2) \quad (7)$$

$$S_{i,j} = \frac{D_i}{D_j}, (i = 1, j = 2) \quad (8)$$

4.1 | Effect of olefin concentration

As shown in Figure 3, the distribution coefficient of 1-octene was much greater than that of n-octane and decreased with increasing olefin concentration but n-octane slightly increased, which may be attributed to the chemical complexation between silver ion and olefin had a more significant contribution to the distribution coefficient and selectivity compared with physical dissolution effect.[36] Moreover, the polarity of 1-octene is greater than that of n-octane (dipole moment: 1-octene (μ = 0.42) > n-octane (μ = 0.07)), which leads to the

physical solubility of 1-octene is also higher than that of n-octane in the polar solvent. So the content of 1-octene in solvent phase was much greater than that of n-octane and got the higher selectivity. However, the complex sites gradually reached saturation[37] as the mass ratio of olefin increased and then the solubility was mainly dominated by the weak physical dissolution and the distribution coefficient of 1-octene decreased. A slight increase for n-octane can be ascribed to the low concentration of n-octane in organic phase in the higher olefin concentration region. When the mass percent of 1-octene was as low as 10 wt.%, the selectivity could achieve 16.74, while it was as high as 90 wt.%, the selectivity only reached 3.75. Therefore, the lower olefin concentration in initio feed, the higher selectivity of 1-octene to n-octane gained.

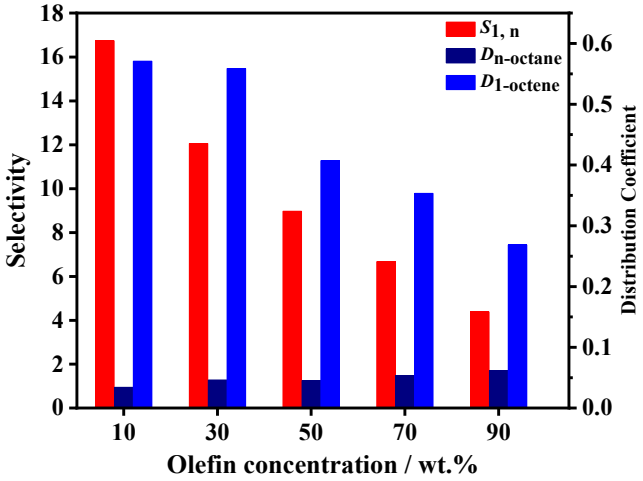

FIGURE 3 Effect of olefin concentration on the distribution coefficient and selectivity of 1-octene to n-octane in the ternary biphasic system, including 11.106 g Ag-DES and 4.48 g C8 with the mass ratio of 1-octene in initio feed ranging from 10 wt.% to 90 wt.% at 25°C

With the reactive extraction experiments data calculated by the mass conservation shown in Table S1, the ternary phase diagram containing 1-octene + n-octane + Ag-DES was depicted as shown in Figure 4. It contains two pairs of partially miscible components and one

pair of completely miscible. The solubility of 1-octene in Ag-DES is greater than that of n-octane.

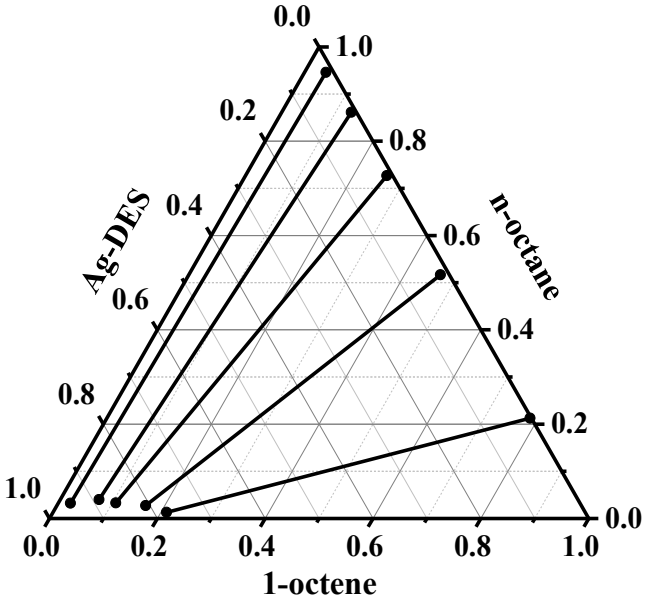

FIGURE 4 The ternary diagram of 1-octene + n-octane + Ag-DES at $T = 298.15 \pm 0.5$K

4.2 | Effect of molar ratio of silver ion to 1-octene

As shown in Figure 5, the distribution coefficient of 1-octene raised with increasing the molar ratio of silver ion to 1-octene, which should be attributed to the more interaction sites for 1-octene with the increasing silver ion concentration.[13] The distribution coefficient of n-octane nearly unchanged due to the limitation of physical solubility in the Ag-DES. Furthermore, the greater the molar ratio of silver ion to olefin, the higher the selectivity of 1-octene to n-octane obtained. However, the mass fraction of 1-octene after the extraction experiment increased firstly from 1:1 to 1:2 and then decreased less than 1:2, which indicates the optimal molar ratio of silver ion to 1-octene is about 1:2. Therefore, the greater silver ion concentration is more favorable for the separation of 1-octene and n-octane and the best separation performance can be acquired at the molar ratio of 1:2.

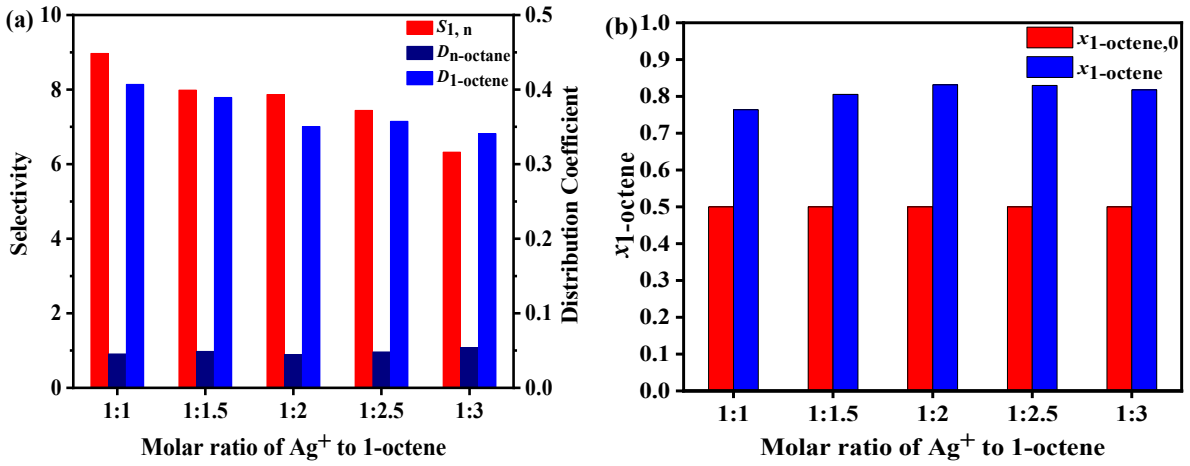

FIGURE 5 Effect of molar ratio of silver ion to 1-octene on (a) the distribution coefficient and selectivity of 1-octene to n-octane; (b) the purification ability of 1-octene in the ternary biphasic system, including 11.106 g Ag-DES and C8 mixture with 50 wt.% olefin and the molar ratio of Ag-DES to 1-octene ranging from 1:1 to 1:3 at 25°C

4.3 | Effect of temperature

The distribution coefficient of 1-octene decreased with the increasing temperature from 10°C as shown in Figure 6, which can be attributed to two reasons. On the one hand, increasing the temperature is conducive to the dissolution and diffusion of organic components in the Ag-DES.[38] On the other hand, increasing the temperature is negative for the chemical complexation between silver ion and olefin because the complexation is an exothermic process.[39] Comparing both of the two reasons, the decreased distribution coefficient of 1-octene indicates that the chemical interaction is dominant. Furthermore, the physical solubility of n-octane showed a slight increase as the temperature rises. Therefore, the selectivity of 1-octene to n-octane totally decreased with increasing temperature. However, when the operating temperature was as low as 0°C, the distribution coefficient of 1-octene and n-octane is much smaller which may be ascribed to the dominant effect of

physical dissolution at such a low temperature. Consequently, the temperature with 10°C is more favorable for the separation of 1-octene from mixture extracted by Ag-DES.

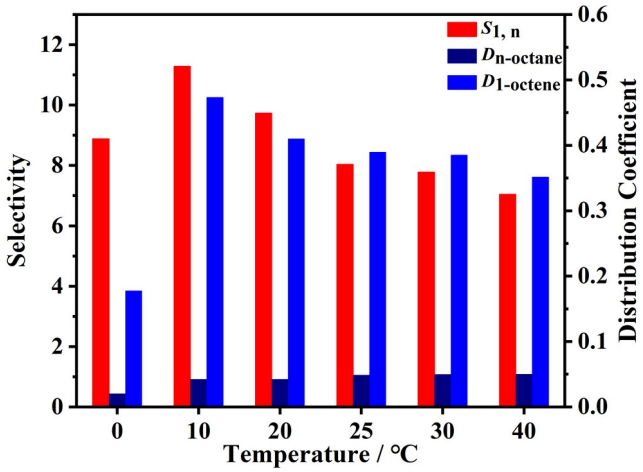

FIGURE 6 Effect of temperature on the distribution coefficient and selectivity of 1-octene to n-octane in the ternary biphasic system, including 11.106 g Ag-DES and 6.72 g C8 mixture with 50 wt.% olefin at the temperature range of 0°C to 40°C

4.4 | Circulation stability

Circulation stability is one of the most important features for an environmental solvent to apply in the separation of α-olefins. As shown in Figure 7, the distribution coefficient and the selectivity of 1-octcene to n-octane remained nearly unchanged, indicating that Ag-DES has a better circulation stability and repeatability for the separation of C8 α-olefin.

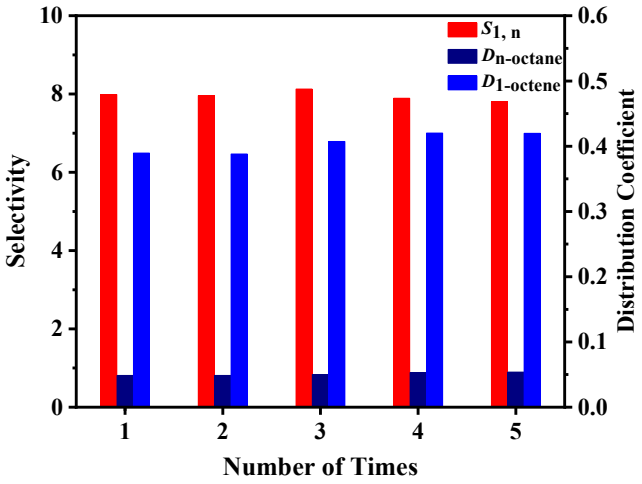

FIGURE 7 Effect of circulation times on the distribution coefficient and selectivity of 1-octene to n-octane in the ternary biphasic system, including 11.106 g Ag-DES and 6.72 g C8 mixture with 50 wt.% olefin at 25°C for five times

4.5 | The extraction performance of Ag-DES compared with ionic liquids

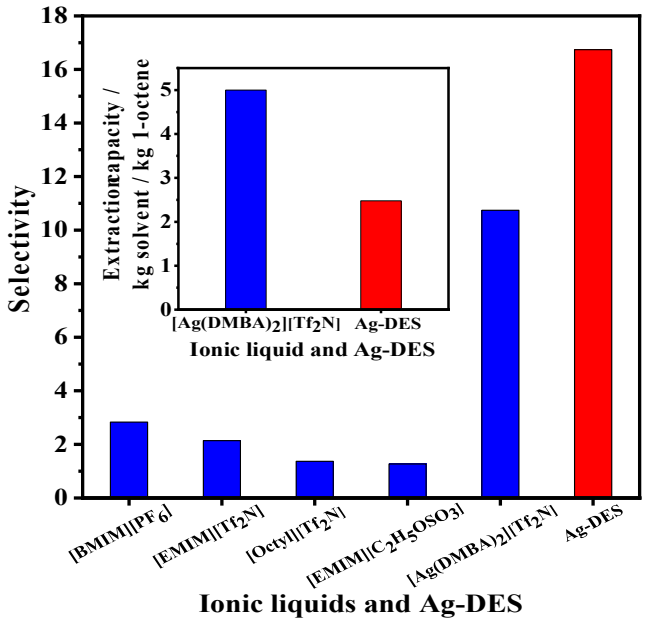

FIGURE 8 The extraction performance of Ag-DES compared with ionic liquids. Red: Ag-DES, Blue: ionic liquids

Compared with the past used ionic liquids, the studied Ag-DES is more favorable for the separation of 1-octene and n-octane as shown in Figure 8. The highest selectivity value 16.74

is higher than 10.74 obtained with $[Ag(DMBA)_2][Tf_2N]$ by Belluomini.[14] The extraction capacity value of approximately 2.48 kg Ag-DES / kg 1-octene is lower than the reported value of 5 kg $[Ag(DMBA)_2][Tf_2N]$ / kg 1-octene. Therefore, the Ag-DES shows better extraction performance than previous silver based and common ionic liquids.

5 | INTERACTION MECHANISM OF Ag-DES WITH 1-OCTENE/ N-OCTANE

5.1 | F-T Raman analysis

Raman analysis was performed to illustrate the interaction mechanism of Ag-DES with 1-octene and n-octane as presented in Figure 9. Comparing the spectrum of the complex with the pure components shown in Figure 9(a), it is obvious that the peak at 1299.64 cm^{-1} appeared in the purple spectrum, which indicates that 1-octene has entered the solvent Ag-DES. If it is only caused by physical dissolution, there should exist a high peak of the carbon-carbon double bond at the position of 1641.95 cm^{-1}. But the fact is that there was only a slight peak at the position of 1640.71 cm^{-1} in their complex, which indicates that there was a very small amount of physical dissolution for 1-octene in the Ag-DES. In addition, the peak of the complex group of silver ion and C=O appeared at the position of 1576.82 cm^{-1}, but compared with the purple spectrum after complexing 1-octene, there was a higher peak at 1579.33 cm^{-1} and a slight red shift peak at 1576.20 cm^{-1}.[40] Previous studies have reported that a new peak of the complex group of silver ion and double bond of olefin appeared at 1585 cm^{-1},[29,41] it can be inferred that the new peak at 1579.33 cm^{-1} should be attributed to such a new group. Because it was too close to distinguish the peak of 1576.82 cm^{-1}, the total area of the peak A and peak B (The stretching vibration peak of the benzene ring at the position of 1513.07 cm^{-1}) was calculated here to confirm the chemical complexation between silver ion and olefin. In

Ag-DES, the peak area ratio A/B was 0.5552, and after combining 1-octene, it obviously increased to 0.7113, which shows that a new peak of complex group overlapped and increased the area. When 1-octene was decomplexed from the complex, the A/B backed to 0.5568. Therefore, the Raman spectrum indicates the generation of chemical complexation between Ag-DES and 1-octene, which further illustrates the stability of the Ag-DES in the process of α-olefins separation. Furthermore, the Raman spectrum of the complex of Ag-DES with n-octane is nearly exactly identical with that of Ag-DES as shown in Figure 9(b), the two characteristic peaks 1304.77 cm^{-1} and 1140.85 cm^{-1} of n-octane didn't appear in the complex spectrum, which suggests that n-octane and Ag-DES are nearly immiscible. According to the extraction experimental results, a small amount of n-octane in the Ag-DES is attributed to the combination of 1-octene and Ag-DES because the two hydrocarbons are miscible. In summary, both of chemical complexation and stronger physical dissolution exist in the complex of Ag-DES with 1-octene, but there is almost no chemical complexation and the physical dissolution between Ag-DES and n-octane. Therefore, as an excellent DES for the separation of 1-octene and n-octane, its cations should have both strong chemical complexation and physical dissolution in order to interact strongly with the 1-octene rather than n-octane.

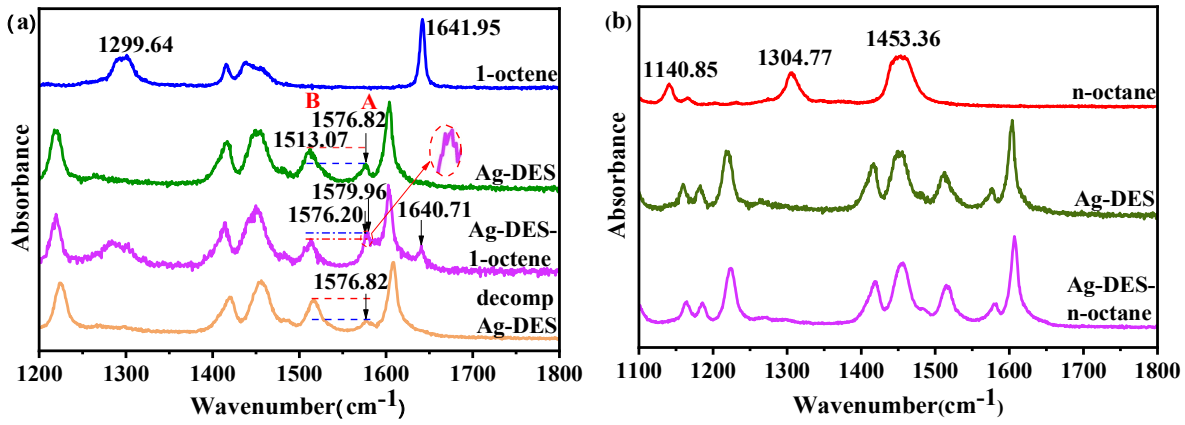

FIGURE 9 Raman spectra of (a) Ag-DES and 1-octene and their complex at the range of 1200-1800 cm^{-1}; (b) Ag-DES and n-octane and their complex at the range of 1100-1800 cm^{-1}

5.2 | Quantum chemistry calculation

5.2.1 | Optimized geometries of Ag-DES and hydrocarbons

The optimized structures of 1-octene and n-octane are shown in Figure S4, the electrostatic potential (ESP) analysis of Ag-DES and its complexes with hydrocarbons are depicted in Figure S5 and their optimized structures were calculated without any imaginary frequency as displayed in Figure 10. The optimized configurations of $AgCF_3SO_3$ and DMBA are shown in Figure 10(a) and (b). When DMBA exists alone, the carbonyl oxygen atoms and the N-methyl hydrogen atoms from two adjacent DMBA molecules can form two C-H…O hydrogen bonds with the same H…O distance of 2.443 Å (which is shorter than the Van der Waals radius of H and O 2.72 Å[42]) and the C-H…O angle of 155.2°. The most stable structure for Ag-DES was optimized as displayed in Figure 10(c) after mixing $AgCF_3SO_3$ and DMBA, which is consistent with the Scheme S1 that the two DMBA molecules are split on both sides by the silver salt and the two C-H…O hydrogen bonds are broken simultaneously, coordination interactions are generated between the free silver ions and the carbonyl oxygen atoms with high negative charge density. The two strong interactions C=O---Ag with the distances of 2.263 Å and 2.294 Å, the C=O---Ag angles of 102.9° and 109.5° and the O---

Ag---O angle of 158.7° exist in the Ag-DES. Comparing with Figure 10(a) and (c), the distance between the silver ion and oxygen atom of the S-O increases from 2.333 Å to 2.448 Å, which suggests that the anion-cation interaction is weakened due to a part of positive charge density of silver ion is occupied by the coordination. The negative charge density of the oxygen atoms of the S=O from the anion of silver salt is higher, which can easily form C-H…O hydrogen bonds with hydrogen atoms from benzene ring (with the C-H…O distances of 2.312 Å and 2.483 Å) and N-methyl (with the C-H…O distances of 2.420 Å and 2.651 Å), etc. Furthermore, it can also be visually indicated by the reduced density gradient (RDG) function and atoms in molecular (AIM) theory that both hydrogen bonds and coordination interactions exist in the synthesis process of Ag-DES as shown in Figure S6 and Figure S7(a), respectively, which play an important role in the stability of solvent.

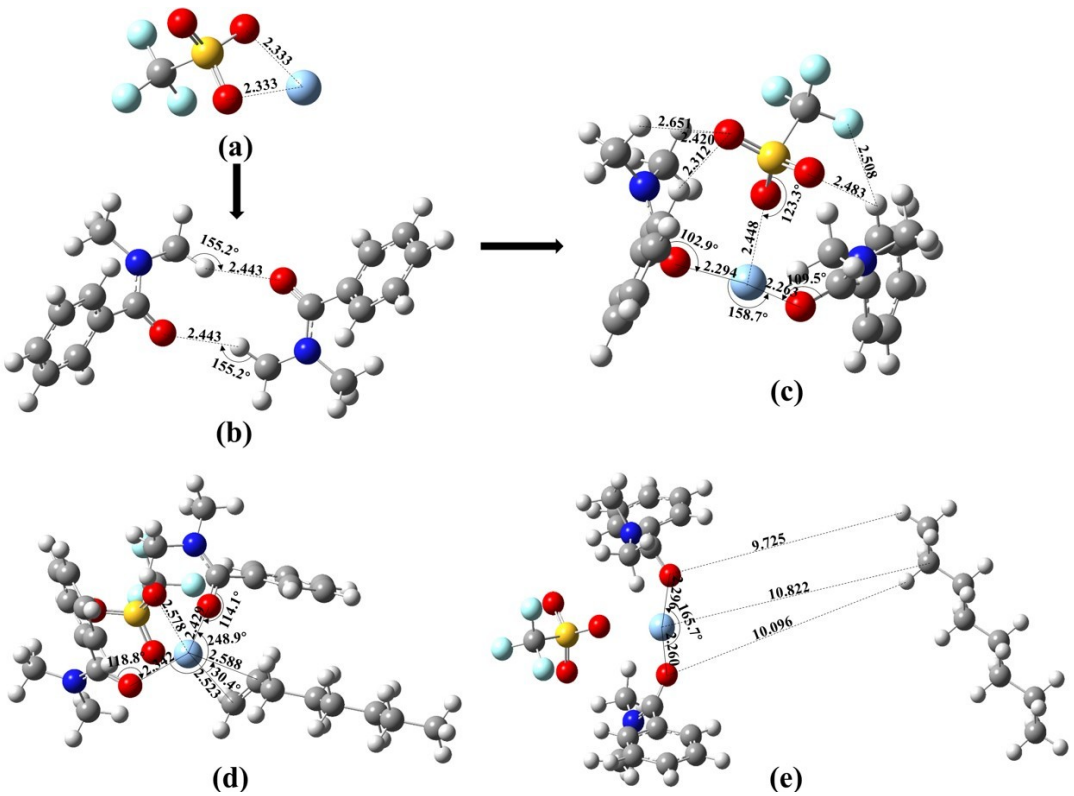

FIGURE 10 The optimized geometry structures for (a) $AgCF_3SO_3$; (b) DMBA; (c) Ag-DES; (d) Ag-DES-1-octene; (e) Ag-DES-n-octane at the M062X/def2tzvp level

The complexes of Ag-DES with 1-octene and n-octane were calculated under the SMD implicit solvent model. As displayed in Figure 10(d), a π bond complex is produced between silver ion and the carbon-carbon double bond of 1-octene with the C=C---Ag distances of 2.523 Å and 2.588 Å, at the same time, the C=O---Ag distances increase from original 2.263 Å and 2.294 Å to 2.342 Å and 2.429 Å, respectively, and the O---Ag---O angle increases from 158.7° to 248.9° and the C=O---Ag angles also increase from 102.9° and 109.5° to 114.1° and 118.8°, respectively, indicating that the complexation between silver ion and C=C is stronger than C=O.[8] Therefore the silver ion moves to the olefin, resulting in the weakness of the complexation between silver ion and carbonyl oxygen. The optimized geometry for the complex of Ag-DES and n-octane is shown in Figure 10(e), the two components are too far to

form weak interactions and the structural parameters of Ag-DES remain nearly unchanged, which means that the interaction strength of 1-octene is much greater than that of n-octane. The results are highly consistent with the AIM analysis depicted in Figure S7, indicating that the lager interaction strength difference between them is the favorable reason for the effective separation of 1-octene.

5.2.2 | Interaction energies analysis

TABLE 2 The interaction energies (kJ/mol) of the complexes Ag-DES(A) – 1-octene/n-octane(B) at the same M062X/def2tzvp level

Ag-DES(A)-hydrocarbon(B)	**Ag-DES-1-octene**	**Ag-DES-n-octane**
E_A/(kJ/mol)	-5431268.05	-5431268.05
E_B/(kJ/mol)	-825915.37	-829141.34
E_{AB}/(kJ/mol)	-6257317.15	-6260520.47
E_{BSSE}/(kJ/mol)	2.30	4.76E-4
E^c_{int}(AB)/(kJ/mol)	-131.42	-111.08
ΔE^c_{int}(AB)/(kJ/mol)	20.35	

Interaction energy is a physical quantity usually obtained through theoretical calculations, which can assist to describe the size of intermolecular interactions.[43] All geometries were optimized at the same theoretical level. The ZPEs of all components can be obtained from Gaussian view 5.0 software package.[44] The interaction energy of the complex AB $E^c_{int(AB)}$ can be calculated by the following Equation (9):

$$E^c_{int(AB)} = E_{(AB)} - E_{(A)} - E_{(B)} + E_{(BSSE)} \quad (9)$$

$E_{(A)}$, $E_{(B)}$ and $E_{(AB)}$ are the ZPEs of A, B and their complex AB, respectively. $E_{(BSSE)}$ is the energy of the basis set superposition error of A and B,[45] which can be calculated through the counterpoise method for more accurate interaction energies.[46] All results are recorded in Table 2. The interaction energy between Ag-DES and 1-octene -131.42 kJ/mol is significantly larger than n-octane -111.08 kJ/mol, and the greater difference between them will inevitably result in a stronger solubility for 1-octene in Ag-DES than n-octane.[20]

6 | PROCESS DESIGN AND ANALYSIS

6.1 | Process design

A reactive extraction process was employed to carry out the separation of 1-octene and n-octane, using Ag-DES as the reactive extractant. As shown in Figure 11, Ag-DES is fed at the upper section of the reactive extractor (T-1) and thoroughly mixed with the C8 mixture fed at the lower section. The organic phase is removed from the top of the reactive extractor, the heavy product Ag-DES and its complex with 1-octene are shifted from the bottom to the flash drum (T-2). 1-octene is withdrawn from the top of the flash as product and Ag-DES is recycled from the bottom to the reactive extractor. Since the boiling point of Ag-DES is much higher, the vapor pressure can be neglected, the recovery of Ag-DES can be accomplished by a flash. Therefore, the reactive extraction separation process contains a reactive extractor and a vacuum flash apparatus for separating 1-octene and recycling Ag-DES, which would be an advanced separation technology compared with other processes.

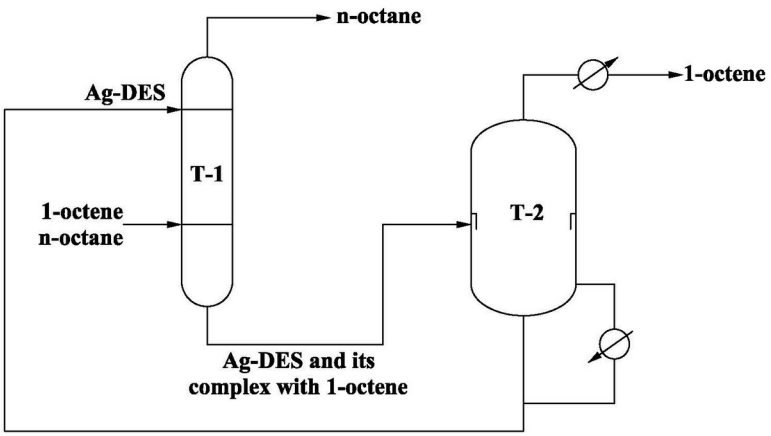

FIGURE 11 Process for reactive extraction 1-octene with Ag-DES

6.2 | Energy consumption analysis

In the reactive extraction separation of 1-octene and n-octane, Ag-DES can be decomplexed by a flash drum under the 65°C and 10 kPa rather than a conventional distillation column. The energy consumption is mainly occurred in the process of recovery of Ag-DES included the sensible heat of heating and latent heat of vaporization because the reactive extraction process has almost no energy consumption, which saves much more energy. The heat duties for the two processes were calculated by using Aspen Plus 8.4 software package with the Wilson property method[47] and the details and results of each simulation process were shown in Table S3. For convenience, seven C8 mixtures containing 1-octene and n-octane with different olefin concentration and the same mass rate of 1 kg/h were injected into the seven distillation columns from different feed stage. The column is operated at 101.3 kPa and the pressure drop on each stage is assumed to be 0.4 kPa. The distillate to feed ratio (D/F) was set as the phase equilibrium results provided in Section 4. Under the premise that varying the mass reflux ratio to guarantee the purity index of the overhead product, the sensitivity analysis of theoretical stages and feed stage was conducted

to obtain the lower heat duty.

Figure 12 shows the energy consumptions of the two processes gained the same composition of product. The energy consumption in the distillation process decreases with the increasing olefin concentration which can be ascribed to the larger reflux ratio to achieve the target mass purity. However, the estimated energy consumption of the reactive extraction process and the yield of α-olefin as a whole increase because of the increased olefin content in the solvent phase with the increasing olefin concentration. Therefore, the energy difference between the two processes gradually becomes smaller. Compared both of them, it is obvious that the reactive extraction separation process is more energy efficient.

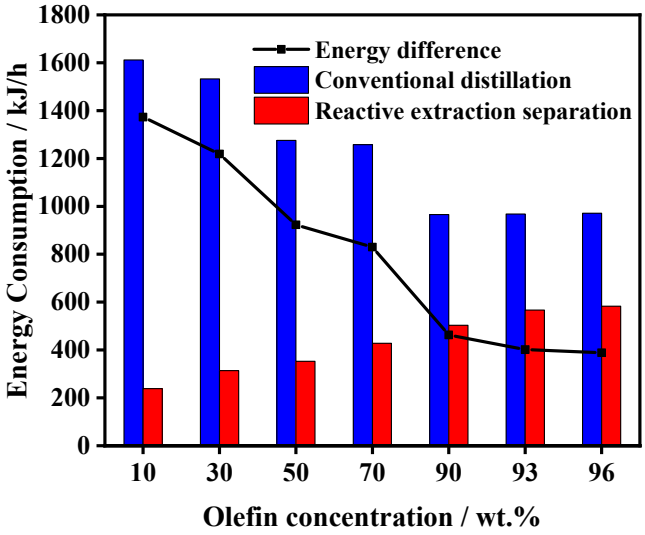

FIGURE 12 Energy consumption in the two processes of conventional distillation and reactive extractive separation

7 | CONCLUSIONS

The first application of DESs in the separation of C8 α-olefin was performed with a novel silver-based deep eutectic solvent consisting of DMBA and $AgCF_3SO_3$. Its structure was well characterized by FT-IR, FT-Raman, ESI-MS and ^1H NMR, which illustrated the successful

preparation of Ag-DES. The separation performance in C8 α-olefin was carried out and showed that the lower olefin concentration and higher silver ion concentration, the larger the selectivity of 1-octene to n-octane obtained. The Ag-DES possessed better performance in the separation of 1-octene/n-octane than those ionic liquids in previous studies, the selectivity could even reach 16.74 for 1-octene to n-octane with the olefin concentration of 10 wt.% in the initial feed at 298.15K. An increase in temperature decreased the selectivity and distribution coefficient for 1-octene because the effect of chemical complexation on selectivity is more significant than physical dissolution. Furthermore, the Ag-DES exhibited an excellent circulation stability, which has great application potential for the separation of long chain α-olefins. In addition, FT-Raman and quantum chemistry calculation were investigated for the determination of interaction between Ag-DES and 1-octene/n-octane. Raman spectra, optimized geometries, interaction energies and AIM topological analysis showed that both the physical dissolution and chemical complexation exist in the complex of Ag-DES with 1-octene, but there is nearly no weak interaction between Ag-DES and n-octane. Therefore, the great interaction difference of Ag-DES with 1-octene and n-octane achieved the excellent separation performance for 1-octene/n-octane. Subsequently, the reactive extraction separation process was proposed for the separation of 1-octene and n-octane, which shows significant energy requirement reduction to obtain the same purity and yield of the α-olefin product compared with the conventional distillate process.

ACKNOWLEDGMENTS

The authors are grateful for the financial support from the National Key R&D Program of China (2018YFB0604900), as well as Key Research and Development program of Ningxia

(2018BDE02057).

REFERENCES

1. Yang RH, Gao RM, Qian Z, Wang YJ. Batch and fixed bed column selective adsorption of C-6, C-8 and C-10 linear alpha-olefins from binary liquid olefin/paraffin mixtures onto 5A and 13X microporous molecular sieves. *Sep Purif Technol.* 2020;230:115884.

2. Wentink AE, Kuipers NJM, de Haan AB, Scholtz J, Mulder H. Olefin isomer separation by reactive extractive distillation: Modelling of vapour-liquid equilibria and conceptual design for 1-hexene purification. *Chem Eng Process-Process Intensif.* 2007;46(9):800-809.

3. Kuipers NJM, Wentinkl AE, de Haan AB, Scholtz J, Mulder H. Functionalized solvents for olefin isomer purification by reactive extractive distillation. *Chem Eng Res Des*. 2007;85(A1):88-99.

4. Eagan NM, Moore BM, McClelland DJ, et al. Catalytic synthesis of distillate-range ethers and olefins from ethanol through Guerbet coupling and etherification. *Green Chem*. 2019;21(12):3300-3318.

5. Sun H, Ren DN, Kong RQ, et al. Tuning 1-hexene/n-hexane adsorption on MOF-74 via constructing Co-Mg bimetallic frameworks. *Micropor Mesopor Mat.* 2019;284:151-160.

6. Piszczek R, Heins B, Hamilton P, et al. Separating linear alpha olefin involves providing a pre-processed product stream comprising linear alpha olefins to first of series of distillation columns, and element of the series of distillation columns comprising a dividing wall column, WO2020114744-A1; 2020.

7. Yang R, Gao R, Wang Y, Qian Z, Luo G. Selective Adsorption of C6, C8, and C10 Linear alpha-Olefins from Binary Liquid-Phase Olefin/Paraffin Mixtures Using Zeolite Adsorbents: Experiment and Simulations. *Langmuir.* 2020;36(29);8597-8609.

8. Faiz R, Li K. Olefin/paraffin separation using membrane based facilitated transport/chemical absorption techniques. *Chem Eng Sci.* 2012;73:261-284.

9. Fallanza M, Ortiz A, Gorri D, Ortiz I. Experimental study of the separation of propane/propylene mixtures by supported ionic liquid membranes containing Ag+–RTILs as carrier. *Sep Purif Technol.* 2012;97:83-89.

10. Safarik DJ, Eldridge RB. Olefin/paraffin separations by reactive absorption: A review. *Ind Eng Chem Res.* 1998;37(7):2571-2581.

11. Liu Z, Zhang LY, Li LF, Zhang SY. Separation of olefin/paraffin by electrodialysis. *Sep Purif Technol.* 2019;218:20-24.

12. Rychlewska K, Kujawski W, Konieczny K. Pervaporative performance of PEBA and PDMS based commercial membranes in thiophene removal from its binary mixtures with hydrocarbons. *Fuel Process Technol.* 2017;165:9-18.

13. Li R, Xing H, Yang Q, et al. Selective Extraction of 1-Hexene Against n-Hexane in Ionic Liquids with or without Silver Salt. *Ind Eng Chem Res.* 2012;51(25):8588-8597.

14. Belluomini GJ, Pendergast JG, Domke CH, Ussing BR. Performance of Several Ionic Liquids for the Separation of 1-Octene from n-Octane. *Ind Eng Chem Res.* 2009;48(24):11168-11174.

15. Dou HZ, Jiang B, Xu M, Zhou JH, Sun YL, Zhang LH. Supported ionic liquid membranes with high carrier efficiency via strong hydrogen-bond basicity for the sustainable and effective olefin/paraffin separation. *Chem Eng Sci.* 2019;193:27-37.

16. Zhang QH, Vigier KD, Royer S, Jerome F. Deep eutectic solvents: syntheses, properties and applications. *Chem Soc Rev.* 2012;41(21):7108-7146.

17. Smith EL, Abbott AP, Ryder KS. Deep Eutectic Solvents (DESs) and Their Applications. *Chem Rev.* 2014;114(21):11060-11082.

18. Esfahani HS, Khoshsima A, Pazuki G. Choline chloride-based deep eutectic solvents as green extractant for the efficient extraction of 1-butanol or 2-butanol from azeotropic n-heptane + butanol mixtures. *J Mol Liq.* 2020;313:113524.

19. Dai YT, van Spronsen J, Witkamp GJ, Verpoorte R, Choi YH. Ionic Liquids and Deep Eutectic Solvents in Natural Products Research: Mixtures of Solids as Extraction Solvents. *J Nat Prod.* 2013;76(11):2162-2173.

20. Liu FJ, Chen W, Mi JX, et al. Thermodynamic and molecular insights into the absorption of H2S, CO2, and CH4 in choline chloride plus urea mixtures. *AIChE J.* 2019;65(5):e16574.

21. Cao YK, Zhang XP, Zeng SJ, Liu YR, Dong HF, Deng C. Protic ionic liquid-based deep eutectic solvents with multiple hydrogen bonding sites for efficient absorption of NH3. *AIChE J.* 2020;66(8):e16253.

22. Faisal M, Haider A, ul Aein Q, Saeed A, Larik FA. Deep eutectic ionic liquids based on DABCO-derived quaternary ammonium salts: A promising reaction medium in gaining access to terpyridines. *Front. Chem. Sci. Eng.* 2019;13(3):586-598.

23. Qin H, Song Z, Zeng Q, Cheng HY, Chen LF, Qi ZW. Bifunctional imidazole-PTSA deep eutectic solvent for synthesizing long-chain ester IBIBE in reactive extraction. *AIChE J.* 2019;65(2):675-683.

24. Li G, Row KH. Utilization of deep eutectic solvents in dispersive liquid-liquid micro-

extraction. *Trac-Trends Anal. Chem.* 2019;120:115651.

25. Ren XY, Zhu XL, Xu CY, et al. The Electrodeposition of Amorphous/Nanocrystalline Ni-Cr Alloys from ChCl-EG Deep Eutectic Solvent. *J Electrochem Soc.* 2020;167(6): 062502.

26. Wadekar PH, Khose RV, Pethsangave DA, Some S. One-Pot Synthesis of Sulfur and Nitrogen Co-Functionalized Graphene Material using Deep Eutectic Solvents for Supercapacitors. *Chemsuschem.* 2019;12(14):3326-3335.

27. Jiang B, Dou HZ, Wang BY, et al. Silver-Based Deep Eutectic Solvents as Separation Media: Supported Liquid Membranes for Facilitated Olefin Transport. *Acs Sustain Chem Eng.* 2017;5(8):6873-6882.

28. Sun YL, Bi HR, Dou HZ, et al. A Novel Copper(I)-Based Supported Ionic Liquid Membrane with High Permeability for Ethylene/Ethane Separation. *Ind Eng Chem Res.* 2017;56(3):741-749.

29. Wang Y, Thompson J, Zhou JJ, et al. Use of water in aiding olefin/paraffin (liquid plus liquid) extraction via complexation with a silver bis(trifluoromethylsulfonyl)imide salt. *J Chem Thermodyn.* 2014;77:230-240.

30. Frisch MJ, Trucks GW, Schlege HB, et al. *Gaussian 09*, Revision C. 01. Gaussian, Inc., Wallingford, CT. 2010.

31. Zhao Y, Truhlar DG. The M06 suite of density functionals for main group thermochemistry, thermochemical kinetics, noncovalent interactions, excited states, and transition elements: two new functionals and systematic testing of four M06-class functionals and 12 other functionals. *Theor Chem Acc.* 2008;120(1-3):215-241.

32. Weigend F, Ahlrichs R. Balanced basis sets of split valence, triple zeta valence and

quadruple zeta valence quality for H to Rn: Design and assessment of accuracy. *Phys Chem Chem Phys*. 2005;7(18):3297-3305.

33. Tian L. Multiwfn: a multifunctional wavefunction analyzer. *J comput chem.* 2012;5(33).

34. Erin R J. Revealing noncovalent interactions. *J Am Chem Soc.* 2010;18(132):6498-6506.

35. Bader RFW. Atoms in molecules. *Acc Chem Res.* 1985;18(1):9-15.

36. Ahosseini A, Sensenich B, Weatherley LR, Scurto AM. Phase Equilibrium, Volumetric, and Interfacial Properties of the Ionic Liquid, 1-Hexyl-3-methylimidazolium Bis(trifluoromethylsulfonyl)amide and 1-Octene. *J Chem Eng Data.* 2010;55(4):1611-1617.

37. Wentink AE, Kockmann D, Kuipers NJM, de Haan AB, Scholtz J, Mulder H. Effect of C6-olefin isomers on pi-complexation for purification of 1-hexene by reactive extractive distillation. *Sep Purif Technol.* 2005;43(2):149-162.

38. Jiang B, Dou HZ, Zhang LH, et al. Novel supported liquid membranes based on deep eutectic solvents for olefin-paraffin separation via facilitated transport. *J Memb Sci.* 2017;536:123-132.

39. Ortiz A, Galan LM, Gorri D, de Haan AB, Ortiz I. Reactive Ionic Liquid Media for the Separation of Propylene/Propane Gaseous Mixtures. *Ind Eng Chem Res.* 2010;49(16):7227-7233.

40. Jung KW, Kang SW. Effect of functional group ratio in PEBAX copolymer on propylene/propane separation for facilitated olefin transport membranes. *Sci Rep.* 2019;9:11454.

41. Sunderrajan S, Freeman BD, Hall CK. Fourier transform infrared spectroscopic characterization of olefin complexation by silver salts in solution. *Ind Eng Chem Res.* 1999;38(10):4051-4059.

42. Bondi A. van der Waals Volumes and Radii. *J Phys Chem A.* 1964;68(3):441-451.

43. Okoshi M, Yamada Y, Komaba S, Yamada A, Nakai H. Theoretical Analysis of Interactions between Potassium Ions and Organic Electrolyte Solvents: A Comparison with Lithium, Sodium, and Magnesium Ions. *J Electrochem Soc.* 2017;164(2):A54-A60.

44. Dennington RD, Keith TA, Millam JM. *GaussView 5*. Gaussian, Inc., Wallingford, CT. 2009.

45. Handy NC. The calculation of small molecular interactions by the differences of separate total energies. Some procedures with reduced errors. *Molecular Physics.* 2002;100(1):63-63.

46. Boys SF, Bernardi F. The calculation of small molecular interactions by the differences of separate total energies. Some procedures with reduced errors (Reprinted from Molecular Physics, vol 19, pg 553-566, 1970). *Mol Phys.* 2002;100(1):65-73.

47. Gao X, Zhao Y, Yuan W, et al. Thermodynamic Fundamentals and Energy Efficiency for the Separation and Highly Valued Utilization of Light Naphtha from Fischer-Tropsch Synthesis. *Ind Eng Chem Res.* 2019;58(21):9118-9126.

SUPPORTING INFORMATION

Scheme for the synthesis of Ag-DES. Tables of liquid-liquid phase equilibrium experimental data, some other topological parameters of BCPs and simulation details and results involved in this work. Figures for the Ag-DES characterizations and quantum chemistry calculation

results.